Research Article | Vol. 12, No. 2 / 1 Feb 2022 / Optical Materials Express 823
Optical Materials EXPRESS

# Probing the effect of a glass network on the synthesis and luminescence properties of composite perovskite glasses [Invited]

ANNA KARAGIANNAKI,[1,2] IOANNIS KONIDAKIS,[1,7] GEORGE KOURMOULAKIS,[1,3] IOANNA DEMERIDOU,[1] JANA DZIBELOVA,[4,5] ARISTIDES BAKANDRITSOS,[4,6] AND EMMANUEL STRATAKIS[1,8]

[1]*Institute of Electronic Structure and Laser (IESL), Foundation for Research and Technology (FORTH) N. Plastira 100, Vassilika Vouton, 70013 Heraklion, Crete, Greece*
[2]*Chemistry Department, University of Crete, Vassilika Vouton, 71003 Heraklion, Crete, Greece*
[3]*Materials Science and Technology Department, University of Crete, Vassilika Vouton, 71003 Heraklion, Crete, Greece*
[4]*Regional Centre of Advanced Technologies and Materials, Czech Advanced Technology and Research Institute (CATRIN) Palacký Univercity, Slechtitelů 27, 78900 Olomouc, Czech Republic*
[5]*Department of Experimental Physics, Faculty of Science, Palacký University Olomouc, 17. Listopadu 12, 771 46 Olomouc, Czech Republic*
[6]*Nanotechnology Centre, Centre of Energy and Environmental Technologies, VŠB–Technical University of Ostrava, 17. listopadu 2172/15, 708 00 Ostrava-Poruba, Czech Republic*
[7]*ikonid@iesl.forth.gr*
[8]*stratak@iesl.forth.gr*

**Abstract:** All-inorganic cesium lead bromide perovskite nanocrystals (PNCs) are highly promising candidates for various optoelectronic and photonic devices. However, poor stability upon exposure to moisture and lead toxicity issues significantly limit their applications. A modern and promising strategy on resolving these issues is the encapsulation of highly luminescent (PNCs) within transparent inorganic oxide glasses. While the encapsulation procedure effect on the development and properties of the so-formed PV-Glasses has been explored in detail, there is lack of understanding the influence of the selected glass composition and network type on the outcome of the synthesis. Herein we report on the synthesis and photoluminescence properties of composite perovskite-glasses upon growing all-inorganic lead halide perovskites within three different types of inorganic oxide glasses. When a silver metaphosphate glass matrix is used it is revealed that the low glass transition temperature of the phosphate glass limits significantly the temperature range of the required post-melting annealing treatment, while the lead salt precursors react with the phosphate entities of the network destroying the stoichiometry of the PNCs. As a result the formation of PNCs is hindered. As a consequence, a double network former borophosphate glass was employed as a suitable host. While annealing treatments at higher temperature were facilitated in this case, it is found that the high silver content becomes an obstacle for the perovskite formation. In view of these findings, cesium lead bromide ($CsPbBr_3$) and cesium lead iodide ($CsPbI_3$) composite perovskite borate glasses were synthesized and found to be suitable hosts. Indeed, such composite glasses exhibit interesting photoluminescence properties that are compared with those of PNCs outside the glass matrix.



## 1. Introduction

All-inorganic lead halide perovskites ($CsPbX_3$, X = Cl, Br, I) have exceptional optoelectronic properties, such as high photoluminescence quantum yields (PLQYs), narrow emission bands that can be adjusted to achieve full visible spectrum coverage. Due to the above, they are candidate material for applications in a wide range of optoelectronic devices such as lasers

#445927 https://doi.org/10.1364/OME.445927
Journal © 2022 Received 18 Oct 2021; revised 24 Nov 2021; accepted 25 Nov 2021; published 1 Feb 2022

Optical Materials EXPRESS

[1,2], photodetectors [3], light emitting diodes (LEDs) [4–6], visible light communication [7], energy conversion and storage [8], photocatalysis platforms [9] and neuromorphic computing systems [10]. On the other hand, due to their ionic nature they are highly sensitive to polar solvents and water, which means they are strongly affected by moisture in the air [11], and sensitive upon temperature variations and light irradiation. These factors significantly hinder their applications. Furthermore, the toxicity of lead has aroused serious environmental and health related concerns [12]. Aiming to improve the stability of perovskite nanocrystals (PNCs) while minimizing environmental concerns, various strategies have been implemented, such as surface modification or the incorporation within host materials. For instance, organic polymers have been used as promising hosts. In particular polymethyl methacrylate [13], polystyrene (PS) [14], and poly(styrene-ethylene-butylene-styrene) [15] have been employed. Even though the encapsulation in polymers enhances PNCs stability, it is only for a short period of time due to degradation and aging of the polymer itself. Moreover, the poor thermal stability of polymer compounds limits significantly their application in high power devices. Finally, upon the incorporation of PNCs within organic polymers, significant spectral shifts and reduction in the photoluminescence (PL) features are induced.

On the other hand, due to their chemical and thermal strength, inorganic oxide glasses seem to resolve the aforementioned limitations, while offering remarkable PL stability of the embedded PNCs [16–30]. In addition, their high transparency in most of the visible range leaves the emission feature of the encapsulated PNCs, almost unaffected. Also, they are relatively easy to make, while being non-toxic. To date, there are two main methods for the encapsulation of PNCs within glass matrices. The most common one involves the simultaneous melting of both perovskite and glass precursors [16–30]. Following the typical quenching for the formation of the glass, the growth of PNCs is achieved by means of additional annealing treatments [16–28], or by laser-assisted crystallization techniques [29–30]. A recently developed alternative approach for the synthesis of perovskite-glasses (PV-Glasses) involves the post-glass melting encapsulation of pre-synthesized PNCs within inorganic oxide glass [31]. Namely, the as prepared PNCs are incorporated within the glass following heat treatments at temperatures near the glass transition temperature ($T_g$). These methods offer remarkable advantages in terms of the development of highly photoluminescence perovskite-based materials of superior stability, while rendering the formation of perovskite periodic patterns feasible [31].

While the effect of the encapsulation procedure on the development and properties of the so-formed PV-Glasses has been explored in detail, there is luck of understanding on the effect of the glass composition and network type on the synthesis outcome. Furthermore, the chemical interactions taking place upon the introduction of perovskite precursors into the melting reaction have not been investigated in detail. In inorganic oxide glasses, the network former structural units connect each other through bridging oxygens, while the amount of terminal oxygens is modified by the quantity of the network modifier components. Upon the addition of network modifiers to the glass system, there is a reduction to the connectivity of the network and the creation of network gaps. For instance, it has been shown that upon the introduction of perovskite precursors to the glass system, lead atoms are bonded to the oxygen ones, while at the same time exist free within the network gaps [23]. Notably only the latter can participate in the formation of the perovskite inside the glass. The necessity of annealing procedures has also been identified. By applying additional post-glass melting heat treatments, the structure of the network becomes less stiff and gives the opportunity of atoms' diffusion to form perovskite crystalline compounds.

Herein, we explore the formation of cesium lead bromide and cesium lead iodide PNCs within three types of inorganic oxide glass matrices. In particular, the 'soft' low glass transition temperature ($T_g$) silver metaphosphate ($AgPO_3$), the double network former silver borophosphate ($xAg_2O$-$yP_2O_5$-$zB_2O_3$), and finally the more rigid sodium borate ($0.25Na_2O$-$0.75B_2O_3$). The selection of these glass families was prompted by two main reasons. First, to investigate the

Optical Materials EXPRESS

effect of silver nanoparticles presence on the chemistry of the formation of PNCs within the glass. Second, for investigating the effect of the glass network type on the growth of PNCs. Results reveal important limitations that need to be considered for the synthesis of PV-Glasses, while shedding light on the chemical interactions among the perovskite components and the glass network formers.

## 2. Experimental procedures

### 2.1. Fabrication of perovskite-glasses

All glasses were developed through conventional melt quenching technique upon mixing and melting together appropriate amounts of the reagents. For the perovskite (PV) phosphate glass family, glasses with nominal composition 0.1PV-0.9$AgPO_3$ were prepared, upon mixing together dry powders of $AgNO_3$, $NH_4H_2PO_4$, $Cs_2CO_3$, $PbBr_2$, NaBr, $PbI_2$, and AgI. $AgNO_3$ and $NH_4H_2PO_4$, are the glass modifier and former compounds, respectively [31], whereas the remaining reagents are perovskite precursors [25]. For the borophosphate system glasses with nominal composition of 0.1PV-0.9(0.5$Ag_2O$-0.3$B_2O_3$-0.2$P_2O_5$) were synthesized upon melting the previous reagents and the proper amount of $B_2O_3$, that acts as a second network former. Finally, composite sodium borate-based PV-Glasses with nominal compositions of 0.05PV-0.95(0.25$Na_2O$-0.75$B_2O_3$) and 0.1PV-0.9(0.25$Na_2O$-0.75$B_2O_3$) were prepared upon melting the previously mentioned reagents upon replacing $AgNO_3$ and $NH_4H_2PO_4$ with the appropriate stoichiometric amounts of $Na_2CO_3$ and $B_2O_3$. The precursors for each glass were mixed thoroughly in a platinum crucible, and melted in an electrical furnace at 450-1100 °C for 30 min. Following splat quenching for the development of glass specimens, additional annealing treatments were performed in order to induce chemical interactions between the perovskite components and the formation of PNCs. As it will be discussed in later Sections, the annealing temperature was varied in accordance with the nature of each composite glass system.

### 2.2. Characterization techniques

A Nicolet Almega XR Micro Raman analysis system equipped with a diode-pumped solid-state laser (DPSS) was used for the PV-Glasses characterization. Excitation wavelength was set to 473 nm. The system consists of a confocal single monochromator spectrometer and utilizes a scanning motorized stage to move around the sample of interest. A 100x Olympus objective lens (with numerical aperture of 0.9) is included for tight focus and data collection in micrometer resolution. Max output power was measured 50mW and controlled via a neutral density filter. The signal is analyzed by a high-resolution grating (2400 lines per mm). SEM was performed on a JEOL 7000 field emission scanning electron microscope with an acceleration voltage of 15 kV. For the XRD measurements an X-Ray Rigaku (D/max-2000) diffractometer was used, which was operated with a continuous scan of Cu Ka1 radiation with λ equal to 1.54056 Å. A backscattering setup was used to capture micro-photoluminescence (-PL) spectra. A SuperK EVO supercontinuum white light source (NKT Photonics) was combined with a SuperK Varia filter (NKT Photonics) to allow wavelength selection. The excitation wavelength for the photoluminescence measurements was 470 nm. The PL signal was analyzed using an iHR-320 spectrometer (Horiba Scientific/Jobin Yvon Technology) in this arrangement. It's a 320 mm focal length (f/4.1 aperture) automated spectrometer with two separate gratings on its turret: 300 g/mm and 1200 g/mm. The monochromator's exit is equipped with a Syncerity multichannel charge-coupled device (CCD) Deep Cooled Camera. A Mitutoyo 50x (NA:0.42, f=200 mm) focuses down to ~1μm the spot size for the sample excitation [31]. Raman spectra were recorded on a DXR Raman microscope (Thermo Scientific, USA) employing a diode laser with an excitation line of 633 nm. The laser power on the sample was set to 2 mW, and the exposition

Optical Materials EXPRESS

time was 2s. Finally, transmission electron microscopy images were obtained by a TEM JEOL 2010 equipped with a LaB6 type emission gun at a voltage of 160 kV.

## 3. Results and discussion

### 3.1. Composite perovskite silver phosphate glasses

Figures 1(a) and (b) present indicative scanning electron microscopy (SEM) surface photos of the silver phosphate glasses prepared, namely the $0.1CsPbBr_3$-$0.9AgPO_3$ and $0.1CsPbI_3$-$0.9AgPO_3$, respectively. It becomes apparent that the incorporation of the perovskite precursors within the phosphate glass does not cause any remarkable structural modification on the surface, for both samples. Raman spectroscopy is employed in order to investigate any structural modifications of the phosphate glass network upon mixing and melting together the PV precursors. Figure 1(c) shows the room temperature Raman spectra of the two composite glasses, along with the corresponding spectrum of pristine $AgPO_3$ glass. The metaphosphate network of the $AgPO_3$ glass consists mainly of chains, which are formed by connected phosphate tetrahedral units with bridging and non-bridging oxygen atoms [32–35]. The main band at ca. 1140 $cm^{-1}$ arises from the symmetric stretching vibration of terminal $PO_2^-$ entities, $\nu_{(s)}(PO_2^-)$, of the network, whereas the broader feature at ca. 670 $cm^{-1}$ is attributed to the symmetric stretching movement of the P-O-P bridges within the phosphate backbone, $\nu_{(s)}$(P-O-P) [32–35].

Notably, inspection of Fig. 1(c) reveals that the incorporation of perovskite precursors introduces a strong shoulder at ca. 1090 $cm^{-1}$, and two more features at 1000 $cm^{-1}$ and 950 $cm^{-1}$. The shoulder at 1090 $cm^{-1}$ originates from the asymmetric formation of pyrophosphate entities, $\nu_{(as)}(PO_3^{2-})$, while the mode at 1000 $cm^{-1}$ is assigned to the corresponding symmetric vibration of the same units, $\nu_{(s)}(PO_3^{2-})$ [32–35]. The latter band at ca. 950 $cm^{-1}$ is attributed to the presence of orthophosphate units, $\nu(PO_4^{3-})$, within the glass matrix [32–35]. These spectroscopic findings imply that the lead salts ($PbBr_2$, and $PbI_2$), react with the phosphate glass network upon heating, for the formation of orthophosphate lead species, $Pb_3(PO_4)_2$. Moreover, the appearance of the characteristic Raman features at 950 $cm^{-1}$ and 1000 $cm^{-1}$ for the two PV-Glasses implies an over modification of the metaphosphate glass network towards a less cross-linked pyrophosphate, w30ith more terminal phosphate units present. Additional evidence for this observation comes from the relative intensities of the two dominant Raman bands at ca. 670 $cm^{-1}$ and 1140 $cm^{-1}$. In particular, the relative intensities of these Raman signatures provide immediate indication if the population of terminal or bridging phosphate units changes at the expense of the other. Notably, the intensity of the latter band relative to the former decreases for the PV-Glasses, indicating the creation of more non-bridging (terminal) oxygen atoms throughout the phosphate network. Inevitably, as the lead salts react with the network, the stoichiometry is spoiled, and the cations of the remaining PV precursors act as network modifiers, i.e. charge balancing the negative charge of non-bridging oxygens. Notably, the formation of PNCs within other phosphate glasses might be perfectly feasible. As for instance, when silver-free phosphate systems are used [28], while introducing additional network formers for stabilizing the network backbone and minimize the interactions with the perovskite precursors during annealing treatments.

Based on the above, it is not surprising that Figs. 1(d) and (e) demonstrate that both composite phosphate glasses fail to exhibit strong photoluminescence (PL) features in the vicinity of 1.4-2.5 eV, as it would be expected from the formation of PNCs with bromine and iodine halogens, i.e. at 2.35 eV and 1.78 eV, respectively (Fig. 1(e)) [16,25]. Moreover, the corresponding absorbance profiles of the pristine $AgPO_3$ glass and the two composite glasses are presented in Fig. 1(f). Inspection of Fig. 1(f) reveals that the composite glasses, on the contrary to the pristine $AgPO_3$ glass, exhibit distinct absorption features at 420-450 nm which are attributed to the presence of silver nanoparticles (AgNPs) [36,37], following the annealing treatments. Notably, in these glasses there is no evidence of the characteristic absorption of PNCs in the visible range [25]. Along similar lines, the corresponding XRD patterns presented in Fig. 1(g) demonstrate the

Optical Materials EXPRESS

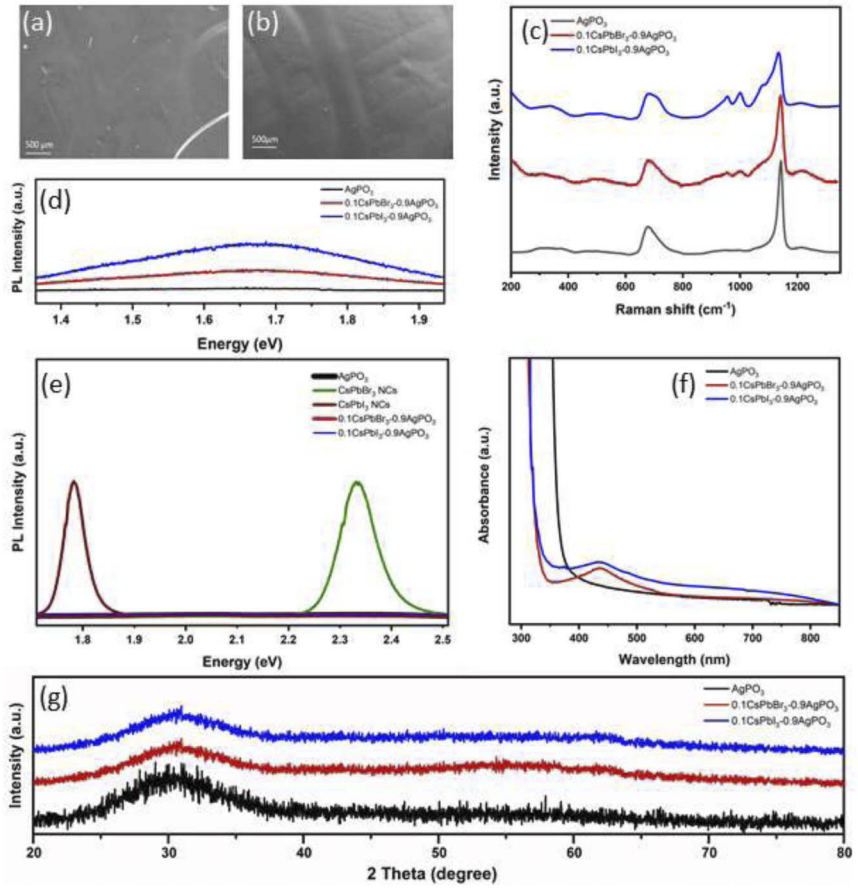


**Fig. 1.** Indicative scanning electron microscopy (SEM) images of the surface of $0.1CsPbBr_3$-$0.9AgPO_3$ (a) and $0.1CsPbI_3$-$AgPO_3$ (b) glasses. Normalized room temperature Raman spectra (c), and room temperature photoluminescence (PL) spectra (d-e). In (e) the PL spectra of the non-encapsulated perovskite nanocrystals (PNCs) have been added for the sake of comparison. (f) Optical absorbance spectra of pristine $AgPO_3$ glass and composite glasses. (g) XRD patterns of pristine $AgPO_3$ glass and the PV-Glasses.

absence of any PV crystalline phase. The formation of PNCs within this glass system is also significantly hindered by another factor. Namely, the $AgPO_3$ glass exhibits a glass transition temperature ($T_g$) of 192 °C [31]. Based on this, during the post-melting annealing treatment of the phosphate PV-Glasses at temperatures above the $T_g$, the phosphate network gains viscosity and becomes active for interactions with the perovskite precursors. Thus, prior to any PV crystal growth, which requires extensive thermal treatment for several hours, the PV precursors react with the host phosphate network, and become unavailable for the formation of PNCs within the glass matrix. After shedding light on these chemical interactions within the silver-based phosphate glass system, glass hosts of higher $T_g$ were employed.

### 3.2. *Composite perovskite silver borophosphate glasses*

In order to overcome the low $T_g$ limitation during post-melting annealing treatment, $B_2O_3$ is introduced as a second network former, for the synthesis of PV-Glasses with nominal composition

Optical Materials EXPRESS

$0.1CsPbI_3$-$0.9(0.5Ag_2O$-$0.3B_2O_3$-$0.2P_2O_5)$. The $T_g$ of the pristine mixed-former host silver-borophosphate glass is 350 °C [38,39]. Figure 2(a) shows a photo of the as prepared glass sample without annealing treatment, whereas Fig. 2(b) depicts an indicative photo after 3 hours of annealing at 320 °C. It becomes apparent that the heat treatment induces a metallic nature of the glass. The corresponding room temperature PL spectra are shown in Fig. 2(c). Likewise to what observed for the phosphate single-network system (Fig. 1), the composite borophosphate glass exhibits only broad fluorescence features arising from the agglomeration of metallic silver nanoparticles (AgNPs) [40–42], which has been observed to intensively occur upon heating silver-containing phosphate glasses near $T_g$. [40–42].

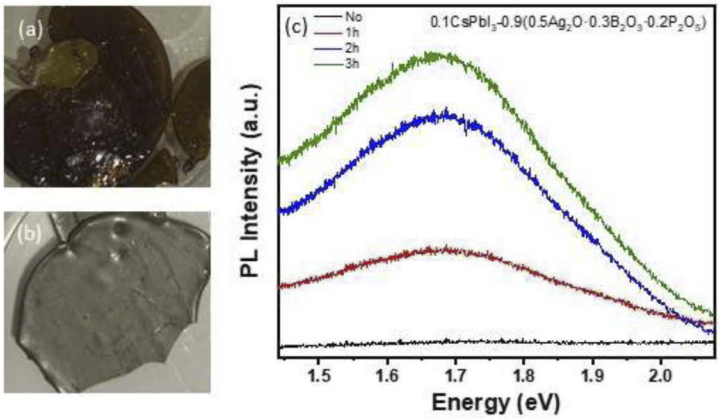


**Fig. 2.** Pictures of $0.1CsPbI_3$-$0.9(0.5Ag_2O$-$0.3B_2O_3$-$0.2P_2O_5)$ composite glass after quenching (a), and after 3 hours of annealing at 320 °C (b). (c) Indicative room temperature photoluminescence (PL) spectra.

### *3.3. Composite perovskite sodium borate glasses*

To avoid the negative effect on the PV crystal phase formation due to the AgNPs agglomeration, we have employed a silver-free sodium borate glass matrix, in which sodium cations act as the network modifiers of the borate glass network. Figures 3(a) and (b) present room temperature PL spectra of $0.05CsPbBr_3$-$0.95(0.25Na_2O$-$0.75B_2O_3)$ and $0.1CsPbBr_3$-$0.9(0.25Na_2O$-$0.75B_2O_3)$ glasses, respectively, annealed for 10 hours at 700 °C. The inset of Fig. 3(a) shows a photo of the former glass under UV light exposure. Remarkably, both PV-Glasses exhibit double peak emission profiles at the vicinity of 1.8 eV. It was demonstrated recently that the often-observed double peak PL spectra of perovskite crystals originates from an extensive self-absorption effect, which is amplified by the high internal reflection within the crystal [43]. In particular, the higher energy level peak at 1.83 eV is the main emission directly outcoupled from the crystals, whereas the lower energy band at 1.79 eV is attributed to additional emission upon multiple internal reflection and self-absorption phenomena [43]. The developed composite $CsPbBr_3$ sodium borate glasses exhibit also characteristic absorbance profiles starting in the vicinity of 650 nm (inset of Fig. 3(b)).

Figure 3(c) shows the PL profiles of additional $0.05CsPbBr_3$-$0.95(0.25Na_2O$-$0.75B_2O_3)$ samples annealed for the same period at 600 °C and 800 °C, whereas the corresponding spectrum of the pristine $0.25Na_2O$-$0.75B_2O_3$ host glass is also shown for the sake of comparison. The latter exhibits no emission, proving that the observed PL features of the composite PV-Glasses arise from the formation of PNCs. Notably, the same double band PL profile is exhibited for all samples independently of the annealing temperature. This finding implies that the reduction or increase of stresses within the host borate glass network upon annealing treatments at higher and

Optical Materials EXPRESS

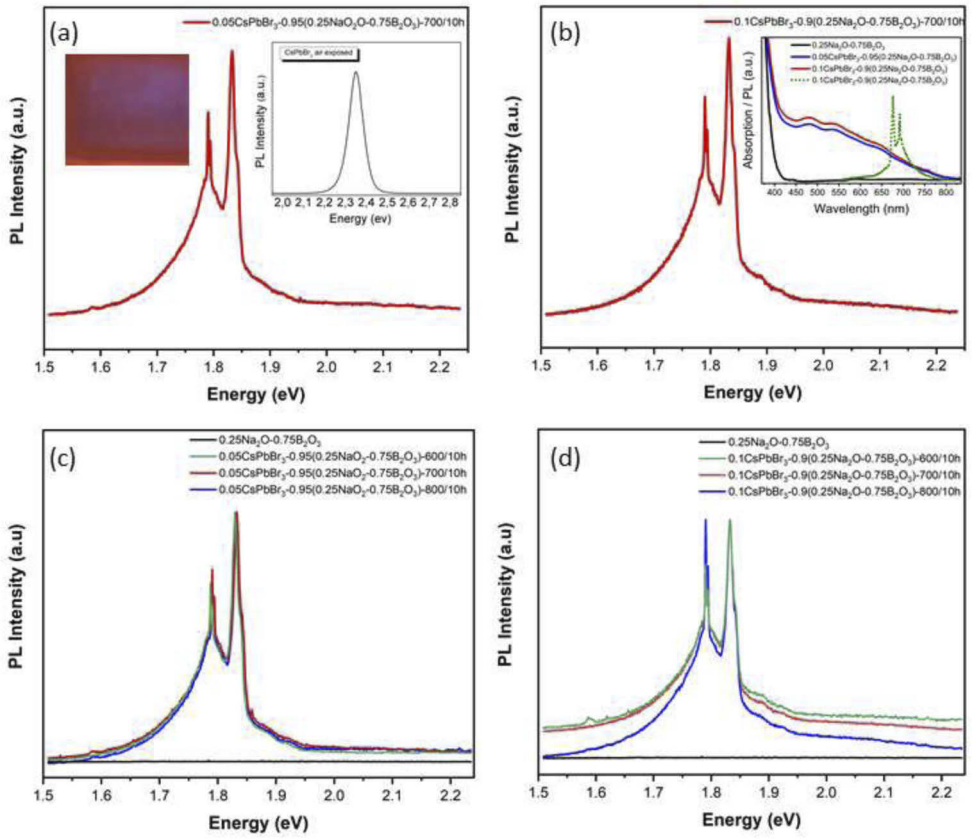


**Fig. 3.** Room temperature photoluminescence (PL) spectra of (a) 0.05$CsPbBr_3$-0.95(0.25$Na_2O$-0.75$B_2O_3$), and (b) 0.1$CsPbBr_3$-0.9(0.25$Na_2O$-0.75$B_2O_3$) composite glasses after 10 hours of annealing at 700 °C, after excitation at 470 nm. The insets of (a) show a picture of the former glass under UV light irradiation, and the corresponding PL of $CsPbBr_3$ PNCs outside the glass [25,31]. The inset of (b) depicts the corresponding optical absorbance profiles of the composite PV-Glasses and the pristine sodium borate glass, while the PL of the 0.1$CsPbBr_3$ PV-Glass is also included. PL spectra of (c) 0.05$CsPbBr_3$-0.95(0.25$Na_2O$-0.75$B_2O_3$), and (d) 0.1$CsPbBr_3$-0.9(0.25$Na_2O$-0.75$B_2O_3$) composite glasses after 10 hours of annealing at various temperatures. The corresponding spectra of the pristine 0.25$Na_2O$-0.75$B_2O_3$ glass is also shown.

lower temperatures, leaves the PL properties of the PNCs unaffected. This provides additional evidence that the obtained double peak PL profile arises only from within the PNCs without any coupling with the borate backbone. On the contrary, the concentration of PNCs affects the relative intensities of the PL bands, particularly for the higher annealing temperatures. Figure 3(d) presents the PL spectra of the 0.1$CsPbBr_3$-0.9(0.25$Na_2O$-0.75$B_2O_3$ glasses annealed at various temperatures. A significant enhancement of the 1.79 eV lower energy band is noticed when compared to the main PL feature at 1.83 eV, implying an enhancement of the self-absorption and internal reflection features when the amount of PNCs is doubled within the host glass matrix.

Figures 4(a) and (b) show indicative transmission electron microscopy (TEM) images of 0.05$CsPbBr_3$-0.95(0.25$Na_2O$-0.75$B_2O_3$) glass, whereas Figs. 4(c) and (d) present the corresponding ones for the 0.1$CsPbBr_3$-0.9(0.25$Na_2O$-0.75$B_2O_3$) sample. Inspection of TEM images reveals that the diameter of $CsPbBr_3$ PNCs ranges between 2 to 10 nm, with an average value

Optical Materials EXPRESS

of 2-3 nm, for both composite PV-Glasses (Fig. 4(e)). Notably, the concentration increase of PNCs within the glass matrix leaves the diameter of the PNCs unaffected. However, the distance between the so-formed PNCs is reduced, as expected, for the composite sample with the higher $CsPbBr_3$ concentration. Aiming to probe the PNCs interactions with the borate glass network, Raman spectroscopy was employed. Figure 4(f) shows room temperature Raman spectra of the pristine borate glass and the two PV-Glasses. All spectra are dominated by two main features, namely a key band at ca. 790 $cm^{-1}$ originating from the boroxol ring vibrations, and a broader profile at ca. 450 $cm^{-1}$ that is attributed to isolated diborate groups [44]. Remarkably, the spectra of the PV-Glasses exhibit a profound enhancement of the Raman modes at the vicinity of 700-735 $cm^{-1}$. Notably, in this range there are no features due to the cesium lead bromide PNCs [31]. Indeed, Raman features in this regime are attributed to the symmetric vibration of metaborate chains [44]. Thus, it is revealed that the growth of PNCs within the glass by means of annealing treatments results to the partial breaking of boroxol rings for the formation of numerous chains that are terminated with negatively charged non-bridging oxygen atoms.

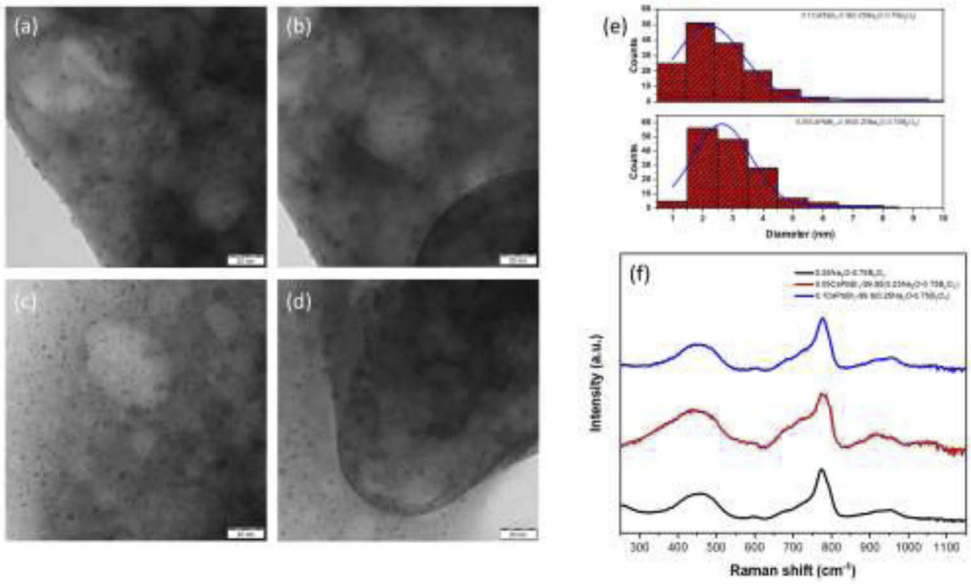


**Fig. 4.** Transmission electron microscopy (TEM) images of cesium lead bromide PNCs within $0.05CsPbBr_3$-$0.95(0.25Na_2O$-$0.75B_2O_3)$ glass (a and b), and within $0.1CsPbBr_3$-$0.1(0.25Na_2O$-$0.75B_2O_3)$ glass (c and d). (e) Histograms of PNCs size distribution in PV-Glasses. (f) Room temperature Raman spectra of the two composite PV-Glasses and the pristine $0.25Na_2O$-$0.75B_2O_3$ glass.

The creation of negatively charged non-bridging oxygen atoms upon perovskite formation provides a plausible explanation for the obtained red shift of the PL features for both $CsPbBr_3$ composite PV-Glasses. Indeed, the main PL band was obtained considerably red-shifted at 1.83 eV (Fig. 3), whereas for typical $CsPbBr_3$ PNCs it is expected at the vicinity of 2.36 eV (inset of Fig. 3(b)) [31]. It has been well recognized that in perovskite compounds of the $ABX_3$ form, cation $A^+$ plays a minor role on the energy bandgap of the crystal. On the contrary, the bandgap is strongly influenced by the anion halide $X^-$ and the nature of the B-X bond [45–47]. Namely, the modification of the halide anion changes the distance and possibly the angle of the X-Pb-X bonds within the $PbX_6$ octahedral of the perovskite structure. In the case of inorganic lead halide perovskites, the bandgap progressively decreases from Cl to Br to I. That is directly related to the smaller electronegativity and larger bond angles of the larger halide atom [45–47]. In the

Optical Materials EXPRESS

PV-Glasses of the present study, the so-formed PNCs are surrounded by negatively charged oxygen atoms. Since there is no extra cation modifier to balance it, the additional negative charge would strongly reduce the electronegativity of the Br-Pb-Br bonds, consequently causing a decrease in the bandgap energy of the encapsulated PNCs.

In addition, Fig. 5(a) depicts the PL spectrum of $0.1CsPbI_3$-$0.1(0.25Na_2O$-$0.75B_2O_3)$ composite glass. The main PL feature at 1.78 eV dominates, while two considerably weaker bands attributed to self-absorption and internal reflections within the PNCs are observed at 1.73 and 1.76 eV. Remarkably, the $CsPbI_3$ PV-Glass exhibits the PL feature exactly to the reported energy value [25,45]. This implies that in case of $CsPbI_3$ the energy bandgap of the encapsulated PNCs remains mostly unaffected from the environment of the host glass network, i.e. in contrast to what was observed for the $CsPbBr_3$ composite PV-Glasses. This finding is rationalized in terms of the fact that the I-Pb-I bonds within the perovskite octahedral will be considerably less vulnerable to the possible presence of additional non-bridging negatively charged entities, due to the low electronegativity of the I atom, i.e. the less electronegative anion of all found in all-inorganic PNCs. The PL emission intensity shows a linear dependence with the excitation power, which is expected for excitonic transitions.

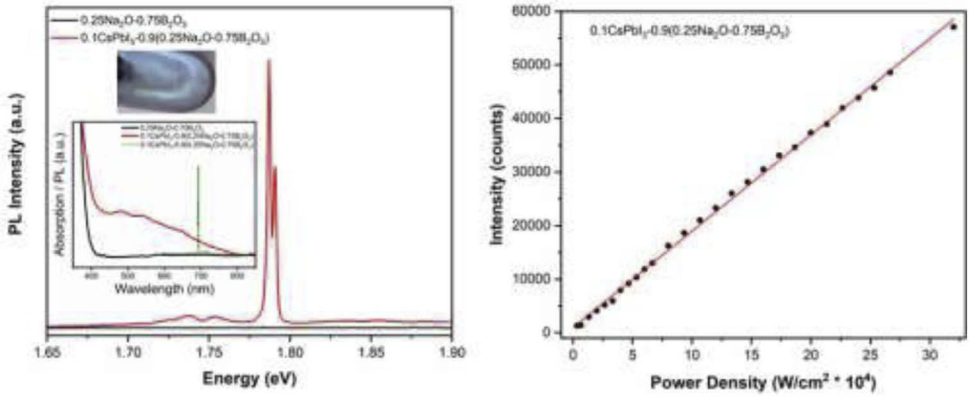


**Fig. 5.** (a) Room temperature photoluminescence (PL) spectra of $0.1CsPbI_3$-$0.9(0.25Na_2O$-$0.75B_2O_3)$ composite glass after 8 hours of annealing at 700 °C. The insets of (a) shows a picture of the glass under UV light irradiation and the corresponding optical absorbance profiles of the composite $CsPbI_3$ PV-Glass and the pristine sodium borate glass, while the PL of the former is also included. (b) Power excitation density dependence of the PL intensity.

Finally, the findings of the present study reveal for the first time the full role of employing extra network former additives of high coordination number on the development of composite inorganic oxide PV-Glasses [16–25]. Typical examples of such compounds are $Sb_2O_3$ and, $Zn(PO_3)_2$. To date, the acknowledged reasons behind the employment of these glass forming components, is the creation of more cross-linked, rigid and expanded host glass network, that will offer a suitable platform for annealing treatments at higher temperatures, i.e. known to favor the growth of PNCs. Notably, the significance of free space and volume within the glass matrix on assisting ion movement has been thoroughly studied [48]. Thus, the expansion of glass network upon employing formers of high coordination ability facilitates further the perovskite growth procedures within glasses upon improving ionic movement. Nevertheless, the findings of the present study highlight another important role of the highly coordinated additives. That is to assist on maintaining the high connectivity of the network and minimize the formation of chain terminal units with negatively charged oxygens that will consequently alter the optical and luminescence properties of the embedded PNCs. On the other hand, single-network former glass systems like the borate of this study, may offer an advanced platform for controllably tailoring

Optical Materials EXPRESS

the optical properties by means of the intentional introduction of negatively charged terminal units, i.e. without the need to change the composition of the perovskite itself.

## 4. Conclusions

In summary, we have explored the formation of all-inorganic lead halide PNCs within three different types of inorganic oxide glasses. First, it was attempted to grow PNCs inside silver metaphosphate glass ($AgPO_3$), which is mainly characterized by its 'soft' phosphate backbone glass network and a low glass transition temperature ($T_g$). While the low $T_g$ appears promising towards reducing fabrication cost, it becomes an obstacle for the PNCs crystallization, since it limits dramatically the temperature range of the post-melting annealing treatment that is essential for the perovskite crystal growth. Moreover the phosphate network is revealed vulnerable under chemical reactions with the lead precursor salts. In order to overcome these issues, we moved to borophosphate glasses which exhibit higher $T_g$ and network connectivity. In that case, the metallic nature of glass due to the high silver content was found to be a drawback for PNCs formation. As a consequence, silver-free borate composite PV-Glasses were fabricated, and showed to exhibit interesting photoluminescent properties attributed to the embedded PNCs. In the case of $CsPbBr_3$ composite glasses, a significant redshift of the PL profile is obtained, due to the PNCs interactions with the negatively charged oxygen atoms of the borate glass network. The latter are introduced as a result of breaking the borate rings of the network upon PNCs growth within the glass. On the contrary, $CsPbI_3$ composite PV-Glasses of the same host matrix exhibit considerably less tuning of the PL band, due to the extreme electronegativity of the iodine atom.

**Funding.** Ministry of Education, Youth and Sports (No. LM2018124); Palacký University Olomouc (IGA_PrF_2021_003); RIS3Crete (TheSmartMat, G.A. KPHP1-0032623).

**Acknowledgements.** This work is partially supported by the project RIS3Crete, TheSmartMat, "Laser-assisted development of composite thermochromic materials for energy smart and safe buildings", G.A. KPHP1-0032623. Student project by Palacký University Olomouc (IGA_PrF_2021_003) is also gratefully acknowledged. Operation of Raman and TEM facilities were partly funded by the Research Infrastructure NanoEnviCz, supported by the Ministry of Education, Youth and Sports of the Czech Republic under Project No. LM2018124.

**Disclosures.** The authors declare no conflicts of interest.

**Data availability.** Data underlying the results presented in this paper are not publicly available at this time but may be obtained from the authors upon reasonable request.

## References

1. F. Deschler, M. Price, S. Pathak, L. Klintberg, D. D. Jarausch, R. Higler, S. Huettner, T. Leijtens, S. D. Stranks, H. J. Snaith, M. Atature, R. T. Phillips, and R. H. Friend, "High photoluminescence efficiency and optically-pumped lasing in solution-processed mixed halide perovskite semiconductors," J. Phys. Chem. Lett. **5**(8), 1421–1426 (2014).
2. W. Gao and S.F. Yu, "Reality or fantasy—Perovskite semiconductor laser diodes," EcoMat **3**, 12077 (2021).
3. Y. H. Lee, I. Song, S. H. Kim, J. H. Park, S. O Park, J. H. Lee, Y. Won, K. Cho, S. K. Kwak, and J. H. Oh, "Perovskite granular wire photodetectors with ultrahigh photodetectivity," Adv. Mater. **32**(32), 2002357 (2020).
4. L. Zhang, C. Sun, and T. He, "High-performance quasi-2D perovskite light-emitting diodes: from materials to devices," *Light Sci Appl* **10**(1), 61 (2021).
5. H. Guan, S. Zhao, H. Wang, D. Yan, M. Wang, and Z. Zang, "Room temperature synthesis of stable single silica-coated $CsPbBr_3$ quantum dots combining tunable red emission of Ag–In–Zn–S for High-CRI white light-emitting diodes," Nano Energy **67**, 104279 (2020).
6. D.D. Yan, S.Y. Zhao, Y.B Zhang, H.X. Wang, and Z.G. Zang, "Highly efficient emission and high-CRI warm white light-emitting diodes from ligand-modified $CsPbBr_3$ quantum dots," OEA **0**(0), 200075 (2021).
7. Q. Mo, C. Chen, W. Cai, S. Zhao, D. Yan, and Z. Zang, "Room temperature synthesis of stable zirconia-coated $CsPbBr_3$ nanocrystals for white light-emitting diodes and visible light communication," Laser Photonics Rev. **15**(10), 2100278 (2021).
8. A. Kostopoulou, K. Brintakis, N. K. Nasikas, and E. Stratakis, "Perovskite nanocrystals for energy conversion and storage," Nanophotonics **8**(10), 1607–1640 (2019).
9. P. Kanhere and Z. Chen, "A review on visible light active perovskite-based photocatalysts," Molecules **19**(12), 19995–20022 (2014).
10. I. Raifuku, Y.-P. Chao, H.-H. Chen, C.-F. Lin, P.-E. Lin, L.-C. Shih, K.-T. Chen, J.-Y. Chen, J.-S. Chen, and P. Chen, "Halide perovskite for low-power consumption neuromorphic devices," EcoMat **9**, 1 (2021).

Optical Materials EXPRESS


11. Z. Zhu, Q. Sun, Z. Zhang, J. Dai, G. Xing, S. Li, X. Huang, and W. Huang, "Metal halide perovskites: stability and sensing-ability," J. Mater. Chem. C **6**(38), 10121–10137 (2018).
12. R. A. Goyer, "Lead toxicity: current concerns," Environ. Health Perspect. **100**, 177–187 (1993).
13. K. Ma, X.-Y. Du, Y.-W. Zhanga, and S. Chen, "In situ fabrication of halide perovskite nanocrystals embedded in polymer composites via microfluidic spinning microreactors," J. Mater. Chem. C **5**(36), 9398–9404 (2017).
14. X. Liang, M. Chen, Q. Wang, S. Guo, and H. Yang, "Ethanol-precipitable, silica-passivated perovskite nanocrystals incorporated into polystyrene microspheres for long-term storage and reusage," Angew. Chem. **131**(9), 2825–2829 (2019).
15. S. N. Raja, Y. Bekenstein, M. A. Koc, S. Fischer, D. Zhang, L. Lin, R. O. Ritchie, P. Yang, and A. Paul Alivisatos, "Encapsulation of perovskite nanocrystals into macroscale polymer matrices: enhanced stability and polarization," ACS Appl. Mater. Interfaces **8**(51), 35523–35533 (2016).
16. S. Yuan, D. Chen, X. Li, J. Zhong, and X. Xu, "In situ crystallization synthesis of $CsPbBr_3$ perovskite quantum dots embedded glasses with improved stability for solid-state-lighting and random upconverted lasing," ACS Appl. Mater. Interfaces **10**(22), 18918–18926 (2018).
17. P. Li, W. Xie, W. Mao, Y. Tian, F. Huang, S. Xu, and J. Zhang, "A new whole family perovskites quantum dots ($CsPbX_3$, X = Cl, Br, I) phosphate glasses with full spectral emissions," J. Alloys. Compd. **817**, 153338 (2020).
18. E. Erol, O. Kıbrıslı, M. C. Ersundu, and A. E. Ersundu, "Size-controlled emission of long-time durable $CsPbBr_3$ perovskite quantum dots embedded tellurite glass nanocomposites," Chem. Eng. J. **401**, 126053 (2020).
19. Y. Liu, W. Chen, J. Zhonga, and D. Chen, "Upconversion luminescence in Yb/Ln (Ln = Er, Tm) doped oxyhalide glasses containing $CsPbBr_3$ perovskite nanocrystals," J. Eur. Ceram. Soc. **39**(14), 4275–4282 (2019).
20. Y. Ye, W. Zhang, Z. Zhao, J. Wang, C. Liu, Z. Deng, X. Zhao, and J. Han, "Highly luminescent cesium lead halide perovskite nanocrystals stabilized in glasses for light-emitting applications," Adv. Optical Mater. **7**(9), 1801663 (2019).
21. Y. Zhu, B. Yang, Q. Lu, Y. Li, M. Shi, and J. Zou, "A cyan emitting $CsPbBr_3$ perovskite quantum dot glass with Bi doping," ECS J. Solid State Sci. Technol. **9**(12), 126003 (2020).
22. X. Liu, E. Mei, Z. Liu, J. Du, X. Liang, and W. Xiang, "stable, low-threshold amplification spontaneous emission of blue emitting $CsPbCl_2Br_1$ perovskite nanocrystals glasses with controlled crystallization," ACS Photonics **8**, 887–893 (2021).
23. B. Yanga, F. Zheng, S. Mei, Z. Chen, Y. Xieb, H. Dai, X. Wei, W. Zhang, F. Xie, Jiaqi Ju, Y. Chu, J. Zou, and R. Guo, "Component regulation and crystallization mechanism of $CsPbBr_3/Cs_4PbBr_6$ perovskite composite quantum dots-embedded borosilicate glass for light emitting application," Appl. Surf. Sci. **512**, 145655 (2020).
24. Y. Du, X. Wang, D. Shen, J. Yuan, Y. Wang, S. Yan, S. Han, Y. Tao, and D. Chen, "Precipitation of $CsPbBr_3$ quantum dots in borophosphate glasses inducted by heat-treatment and UV-NIR ultrafast lasers," Chem. Eng. J. **401**, 126132 (2020).
25. D. Chen, S. Yuan, X. Chen, J. Li, Q. Mao, X. Lia, and J. Zhonga, "$CsPbX_3$ (X = Br, I) perovskite quantum dot embedded low-melting phosphosilicate glasses: controllable crystallization, thermal stability and tunable emissions," J. Mater. Chem. C **6**(25), 6832–6839 (2018).
26. X. Di, Z. Hu, J. Jiang, M. He, L. Zhou, W. Xiang, and X. Liang, "Use of long-term stable CsPbBr3 perovskite quantum dots in phospho-silicate glass for highly efficient white LEDs," Chem. Commun. **53**(80), 11068–11071 (2017).
27. Z. Yang, H. Zhang, Z. Fang, J. Yi b, P. Song, X. Yu, D. Zhou, J. Qiu, and X. Xu, "One-step precipitated all-inorganic perovskite QDs from amorphous media for backlighting display and reproducible laser-driven white lighting," Chem. Eng. J. **427**, 131379 (2022).
28. B. Ai, C. Liu, J. Wang, J. Xie, J. Han, and X. Zhao, "Precipitation and optical properties of $CsPbBr_3$ quantum dots in phosphate glasses," J. Am. Ceram. Soc. **99**(9), 2875–2877 (2016).
29. Y. Hu, W. Zhang, Y. Ye, Z. Zhao, and C. Liu, "Femtosecond-laser-induced precipitation of $CsPbBr_3$ perovskite nanocrystals in glasses for solar spectral conversion," ACS Appl. Nano Mater. **3**(1), 850–857 (2020).
30. X. Huang, Q. Guo, S. Kang, T. Ouyang, Q. Chen, X. Liu, Z. Xia, Z. Yang, Q. Zhang, J. Qiu, and G. Dong, "Three-dimensional laser-assisted patterning of blue-emissive metal halide perovskite nanocrystals inside a glass with switchable photoluminescence," ACS Nano **14**(3), 3150–3158 (2020).
31. I. Konidakis, K. Brintakis, A. Kostopoulou, I. Demeridou, P. Kavatzikidou, and E. Stratakis, "Highly luminescent and ultrastable cesium lead bromide perovskite patterns generated in phosphate glass matrices," Nanoscale **12**(25), 13697–13707 (2020).
32. R.F. Bartholomew, "Structure and properties of silver phosphate glasses- infrared and visible spectra," J. Non-Cryst. Sol. **7**(3), 221–235 (1972).
33. A. Fontana, F. Rossi, C. Armellini, G. Dangelo, G. Tripodo, and A. Bartolotta, "Low-temperature optical and thermal properties of AgI-based phosphate glasses," Philos. Mag. B **79**(11-12), 2073–2080 (1999).
34. R. K. Brow, "Review: the structure of simple phosphate glasses," J. Non-Cryst. Solids **263M**, 1–28 (2000).
35. D. Palles, I. Konidakis, C. P. E. Varsamis, and E. I. Kamitsos, "Vibrational spectroscopic and bond valence study of structure and bonding in Al2O3-containing AgI–AgPO3 glasses," RSC Adv. **6**(20), 16697–16710 (2016).
36. D. A. Klyukin, V. D. Dubrovin, A. S. Pshenova, S. E. Putilin, T. A. Shakhverdov, A. N. Tsypkin, N. V. Nikonorov, and A. I. Sidorov, "Formation of luminescent and nonluminescent silver nanoparticles in silicate glasses by near-infrared

Optical Materials EXPRESS

femtosecond laser pulses and subsequent thermal treatment: the role of halogenides," Opt. Eng. **55**(6), 067101 (2016).
37. A. Zhang, J. Zhang, and Y. Fang, "Photoluminescence from colloidal silver nanoparticles," J. of Luminescence **128**, 1635 (2008).
38. A. Magistris, G. Chiodelli, and M. Duclot, "Silver borophosphate glasses: Ion transport, thermal stability and electrochemical behaviour," Solid State Ionics **9**, 611–615 (1983).
39. S. Kabi and A. Ghosh, "Mixed glass former effect in AgI doped silver borophosphate glasses," Solid State Ionics **262**, 778–781 (2014).
40. I. Konidakis and S. Pissadakis, "Optical spectra tuning of all-glass photonic bandgap fiber infiltrated with silver fast-ion-conducting glasses," Materials **7**(8), 5735–5745 (2014).
41. I. Konidakis, S. Psilodimitrakopoulos, K. Kosma, A. Lemonis, and E. Stratakis, "Effect of composition and temperature on the second harmonic generation of in silver phosphate glasses," Opt. Mater. **75**, 796 (2018).
42. A.S. Sarkar, I. Konidakis, I. Demeridou, E. Serpetzoglou, G. Kioseoglou, and E. Stratakis, "Robust B-exciton emission at room temperature in few layers of $MoS_2$:Ag nanoheterojunctions embedded into a glass matrix," Sci. Rep. **10**, 15697 (2020).
43. K. Schötz, A.M. Askar, W. Peng, D. Seeberger, T.P. Gujar, M. Thelakkat, A. Köhler, S. Huettner, O.M. Bakr, K. Shankar, and F. Panzer, "Double peak emission in lead halide perovskites by self-absorption," J. Mater. Chem. C **8**(7), 2289–2300 (2020).
44. A.K. Yadav and P. Singh, "A review of the structures of oxide glasses by Raman spectroscopy," RSC Adv. **5**(83), 67583–67609 (2015).
45. L. Protesescu, S. Yakunin, M.I. Bodnarchuk, F. Krieg, R. Caputo, C.H. Hendon, R.X. Yang, A. Walsh, and M.V. Kovalenko, "Nanocrystals of cesium lead halide perovskites ($CsPbX_3$, X = Cl, Br, and I): novel optoelectronic materials showing bright emission with wide color gamut," Nano Lett. **15**(6), 3692–3696 (2015).
46. E.Y. Tiguntseva, G.P. Zograf, F.E. Komissarenko, D.A. Zuev, A.A. Zakhidov, S.V. Makarov, and Y.S. Kivshar, "Light emitting halide perovskite nanoantennas," Nano Lett. **18**(2), 1185–1190 (2018).
47. C.T. Crespo, "The effect of the halide anion on the optical properties of lead halide perovskites," Sol. Energy Mater. Sol. Cells **195**, 269–273 (2019).
48. M.D. Ingram, C.T. Imrie, I. Konidakis, and S. Voss, "Significance of activation volumes for cation transport in glassy electrolytes," Phys. Chem. Chem. Phys. **6**(13), 3659–3662 (2004).